

OPEN ACCESS

Polyaniline/clay Nanocomposites: Preparation, Characterization and Electrochemical Properties

To cite this article: B Vijayakumar *et al* 2015 *IOP Conf. Ser.: Mater. Sci. Eng.* **73** 012112

View the [article online](#) for updates and enhancements.

Related content

- [Test of Ferroelectricity in Non-stretched Poly\(vinylidene fluoride\)/Clay Nanocomposites](#)
Eiji Yamada, Akihiro Nishioka, Hideshige Suzuki *et al.*
- [Effect of Processing Variables on Tensile Modulus and Morphology of Polyethylene/Clay Nanocomposites Prepared in an Internal Mixer](#)
O Ujianto, M Jollands and N Kao
- [Novel thermoplastic starch-clay nanocomposite foams](#)
Meng Chen, Biqiong Chen and Julian R G Evans

Recent citations

- [Fen Ran and Yongtao Tan](#)
- [MnO₂/mont K10 composite for high electrochemical capacitive energy storage](#)
Vijayakumar Badathala and Justin Ponniah

Polyaniline/clay Nanocomposites: Preparation, Characterization and Electrochemical Properties

B Vijayakumar^{1,*}, K O Anjana² and G Ranga Rao¹

¹ Department of Chemistry, Indian Institute of Technology Madras, Chennai-600036, India

² Department of Chemistry, National Institute of Technology Calicut, Kozhikode-673601, India

E-mail: badathala@rediffmail.com

Abstract. Preparation of polyaniline (PAni)/clay nanocomposites by reacting aniline with ammonium persulphate in presence of clay at 0-5 °C for 12 h. The composites were characterized by X-ray diffraction, infrared spectroscopy, UV-vis diffuse reflectance spectroscopy and thermogravimetric analysis for their physicochemical properties. Morphology was studied by scanning electron microscopy. The electrochemical studies of PAni/clay nanocomposites were carried out using cyclic voltammetry in 0.5 M H₂SO₄ aqueous electrolyte. The PAni/clay nanocomposites showed specific capacitances of 415–455 Fg⁻¹ at a scan rate of 10 mVs⁻¹.

1. Introduction

Polymer/clay nanocomposites have attracted great interest, because they exhibit remarkable improvement in materials properties such as mechanical, thermal, electrical and optical properties when compared with virgin polymer or conventional micro- and macro-composites. The physical mixture of a polymer and clay may not form a nanocomposite. This situation is analogous to polymer blends, and in most cases separation into discrete phases takes place. In immiscible systems, which typically correspond to the more conventionally filled polymers, the poor physical interaction between the organic and the inorganic components leads to poor mechanical and thermal properties. In contrast, strong interactions between the polymer and clay in polymer/clay nanocomposites lead to the organic and inorganic phases being dispersed at the nanometer level. As a result, nanocomposites exhibit unique properties not shared by their micro counterparts or conventionally filled polymers [1–4]. The natural clays are hydrophilic in nature and hence incompatibility between clay and hydrophobic polymer matrix to obtain a polymer/clay nanocomposite. However, in this state, clays are miscible with hydrophilic polymers, such as poly (ethylene oxide) (PEO) [5], or poly (vinyl alcohol) (PVA) [6]. To render clays miscible with other polymer matrices, one must convert the normally hydrophilic silicate surface to an organophilic one, making the intercalation of many engineering polymers possible. Generally, this can be done by ion-exchange reactions with cationic surfactants including primary, secondary, tertiary, and quaternary alkylammonium or alkylphosphonium cations. Alkylammonium or alkylphosphonium cations in the organosilicates lower the surface energy of the inorganic host and improve the wetting characteristics of the polymer matrix, and result in a larger interlayer spacing. Additionally, the alkylammonium or alkylphosphonium cations can provide functional groups that can react with the polymer matrix, or in some cases initiate the polymerization of monomers to improve the strength of the interface between the inorganic and the polymer matrix [7, 8]. The polymer/clay nanocomposite is obtained when a polymer intercalates in the interlamellar region of clays separates and gets dispersed in polymer matrix [9].

* Corresponding author. Current address: Department of Chemistry, Vel Tech High Tech Dr. Rangarajan Dr. Sakunthala Engineering College, Avadi, Chennai-600 062, India. E-mail: badathala@rediffmail.com, badathala@yahoo.com



Polyaniline is known for more than a century and is potentially one of the most useful conducting polymers because of its facile synthesis, environmental stability, and simple acid/base doping/dedoping chemistry [10]. The present research work deals with the modification of clays to hydrophobic and latter use them in the insitu polymerization to obtain polyaniline/clay nanocomposites. The polyaniline/clay nanocomposites are characterized for their physico-chemical and electrochemical properties.

2. Experimental

2.1 Materials and methods

Smectite rich clay sample from Bhuj area, Gujarat has been used in this study. The composition of the smectite rich clay sample was found to be 53.44% SiO₂, 16.12% Al₂O₃, 13.65% Fe₂O₃, 2.84% MgO, 2.31% Na₂O, 0.27% K₂O, 1.28% CaO, 1.24% TiO₂, 0.02% Cr₂O₃, 0.11% MnO, 0.01% NiO, 0.04% P₂O₅, 0.16% S, and 8.03% ignition loss. The cation exchange capacity (CEC) of the clay was found to be 0.98 meq per g [11]. The other reagents were purchased from Sd-fine, Loba, AVRA, and SRL, India and used as received. X-ray powder diffraction (XRD) data were collected on a Bruker AXS D8 Discover diffractometer with Cu K α radiation ($\lambda = 1.5418 \text{ \AA}$). The IR spectra were recorded in the range of 450-4000 cm⁻¹ on a Perkin-Elmer FTIR spectrometer using KBr pellet. UV-Vis diffuse reflectance (DR) spectra were recorded on JASCO V-530 UV-Vis spectrophotometer. The thermogravimetric analysis (TGA) was conducted on a Perkin-Elmer TGA-7 analyzer in air with a heating rate of 20 °C min⁻¹ from room temperature to 800 °C. Field emission scanning electron microscopic/energy dispersive spectroscopic (FE-SEM/EDS) studies were done in Jeol microscope model JSM-6700F.

For electrochemical characterization, electrodes were fabricated on a high purity nickel as a current collector. The nickel was polished with successive grades of emery paper, sonicated and washed thoroughly with detergent and distilled water. 80 wt % of polyaniline/clay nanocomposite, 15 wt % of acetylene black, and 5 wt % of polyvinylidene fluoride (PVDF) were ground in a mortar. Few drops of *n*-methyl pyrrolidinone (NMP) were added to make syrup. This was then coated on to the pretreated nickel foil and dried at 60 °C under reduced pressure for 12 h. The electrochemical studies were performed on a CHI 7081C electrochemical workstation using a three electrode-configuration-cell consisting of polyaniline/clay nanocomposite as the working electrode, platinum foil (1 × 2 cm²) as a counter electrode and SCE as reference electrode, all dipped in 0.5 M H₂SO₄ aqueous electrolyte.

3. Results and discussion

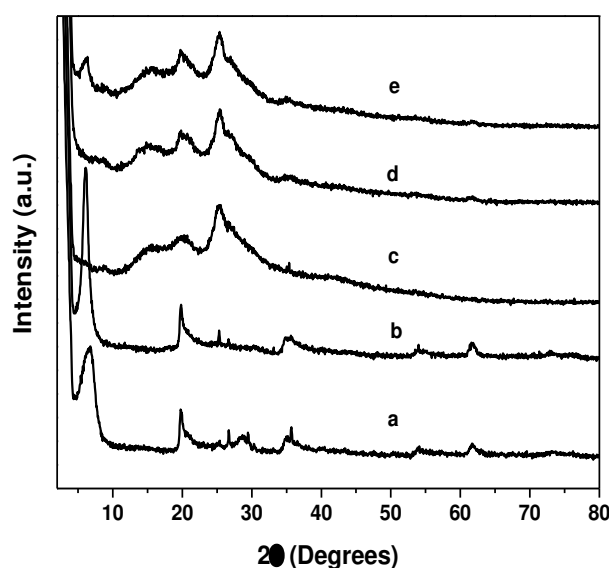


Fig. 1 PXRD patterns of (a) IB, (b) OMIB, (c) PANi, (d) PANi/IB and (e) PANi/OMIB.

3.1 XRD

Fig. 1 shows powder XRD patterns of Indian bentonite (IB), organically modified Indian bentonite (OMIB), PANi, PANi/IB, and PANi/OMIB. The peak at 6.75° in Fig. 1a corresponds to the periodicity in the direction of (0 0 1) of the IB sample. The XRD pattern of OMIB showed peak at 18.64 \AA which is due to the grafting of CTAB to silanol groups within the interlayer where the silica framework is in contact with the clay layers [12]. The peak is shifted due to the interaction between PANi and the modified clay in PANi/OMIB (Fig. 1e). The d-spacing in the direction of (0 0 1) of the IB sample is 13.07 \AA , OMIB is 18.64 \AA and that of PANi/OMIB is 14.60 \AA respectively. The PANi/IB (Fig. 1d) showed very small peaks corresponding to clay due to its lower weight percent in the sample. These results demonstrate that the conducting PANi/clay nanocomposites are of the order of nanoscale size.

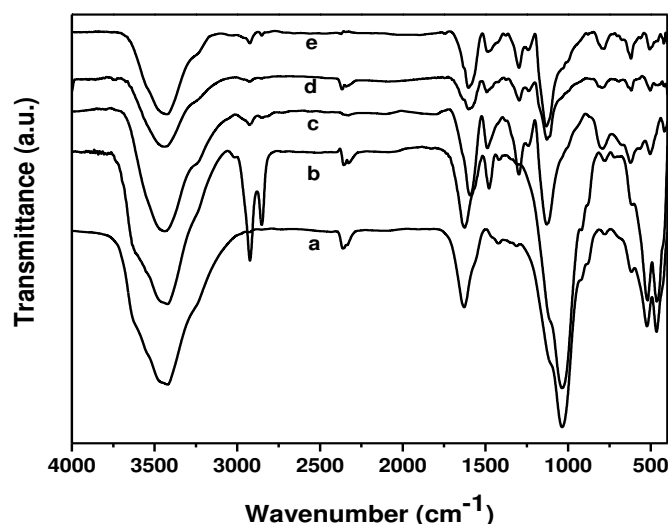


Fig. 2 FTIR spectra of (a) IB, (b) OMIB, (c) PANi, (d) PANi/IB and (e) PANi/OMIB.

3.2 FTIR

Fig. 2 shows FTIR spectra of IB, OMIB, PANi, PANi/IB, and PANi/OMIB. The infrared spectrum of PANi (Fig. 2c) shows broad band centred at 3451 cm^{-1} corresponds to N-H stretching with hydrogen bonded amino groups and free O-H stretching vibration and is attributed to the N-H stretching vibrations of the leucoemeraldine component. The characteristic absorption band observed for PANi/IB and PANi/OMIB (Fig. 2d & e) at 3451 cm^{-1} and 1597 cm^{-1} are assigned to the N-H stretching vibration mode, and NH_2 deformation in aniline unit respectively. The absorption bands at 2915 cm^{-1} and 2829 cm^{-1} are assigned to the aromatic sp^2 hybridized C-H stretching vibration mode and aliphatic hydrocarbon C-H stretching due to $-\text{CH}_2-$ group in OMIB, PANi, PANi/IB and PANi/OMIB. The absorption bands observed at 1597 & 1479 cm^{-1} in PANi are assigned to the non-symmetric vibration mode of C=C in quinoid and benzenoid ring system in PANi. The C-N stretching vibration mode in aromatic amine nitrogen (quinoid system) in doped PANi is found at 1297 cm^{-1} , corresponding to the oxidation or protonation state. The IR peak at 1236 cm^{-1} is attributed to C-N stretching vibration mode in benzenoid ring system of PANi due to the conducting protonated form. In plane vibration of C-H bending mode in N=Q=N, Q-N+H-B or B-N+H-B (where Q = quinoid and B = benzenoid) is observed at 1113 cm^{-1} . The presence of this absorption band is expected due to the polymerization of PANi, i.e., polar structure of the conducting protonated form. The absorption band at 799 cm^{-1} is attributed to the aromatic ring and out of plane C-H deformation vibrations for 1, 4-disubstituted aromatic ring system [13].

The characteristic bands corresponding to clay are 1038 (Si-O), 911 (Al-OH) and 525cm^{-1} (Si-O-Al). The Si-O-Si stretching vibration of the clay matrix (1038 cm^{-1}) present in the montmorillonite [14] is merged with the peak at 1113 cm^{-1} in the composites and this peak appeared as a broad one. The FTIR peak at 1038 cm^{-1} for the clay corresponds to the internal SiO_4 tetrahedra, especially the Si-O-Si chain structure. The decrease in broadening of FTIR bands in the range $3062 - 3451\text{ cm}^{-1}$ may be due to covalent and hydrogen bonding between $-\text{NH}_2$ and $-\text{OH}$ group of PANi and clay respectively.

3.3 UV-Vis DR study

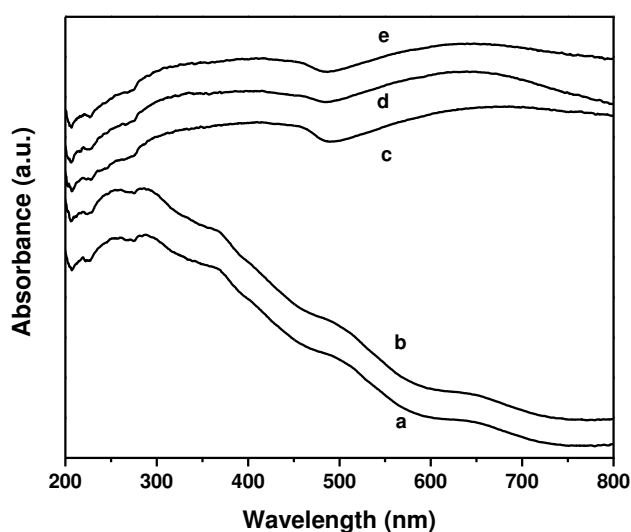


Fig. 3 UV-Vis spectra of (a) IB, (b) OMIB, (c) PANi, (d) PAni/IB and (e) PAni/OMIB.

Fig. 3 shows the UV-vis absorption spectra of IB, OMIB, PANi, PAni/IB, and PAni/OMIB. Two absorption bands are observed in the wavelength region from 315 to 350 nm and a small band at 578 to 712 nm for the PANi (Fig. 3c). PANi always exhibits a $\pi-\pi^*$ transition, usually closer to 315 nm [54]. Partially oxidized PANi and its oligomers display an additional absorption at around 712 nm associated with the quinoid (oxidized) units [15]. These peaks are characteristic of the PANi emeraldine base [14, 16] and indicate that nanostructured PANi composites are stabilized in the emeraldine base redox state. The peak at 315 nm is attributed to $\pi - \pi^*$ transition of benzenoid rings and the peak at 712 nm is attributed to the charge transfer excitation of the quinoid structure. In the spectra of IB and OMIB, peaks are observed in the regions at 248-262 nm related to Fe^{3+} ions in octahedral coordination (Fig. 3a & b). PAni/IB and PAni/OMIB nanocomposites show clear similarity in their UV-vis spectra particularly with the presence of the absorption maxima at 315 and 610 nm which is associated with the stabilization of the composite in the emeraldine form. Comparison of the PANi and PAni/clay nanocomposites spectra shows that clay stabilizes the polyanilines in its emeraldine form.

3.4 TGA

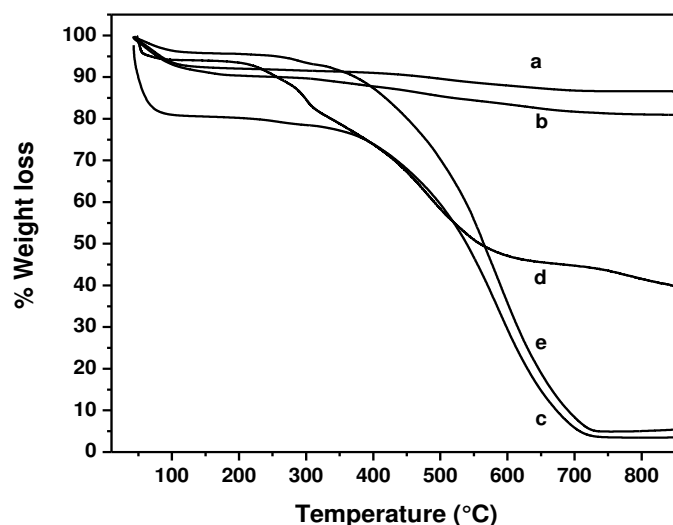


Fig. 4 TG plots of (a) IB, (b) OMIB, (c) PANi, (d) PANi/IB and (e) PANi/OMIB.

Fig. 4 shows TG plots of IB, OMIB, PANi, PANi/IB and PANi/OMIB. The thermogram of PANi indicates three major stages of weight loss (Fig. 4c). In the first stage, 3-4% weight loss at temperature up to 100 °C is associated with the loss of water molecules from the polymer matrix [17]. The weight loss at second stage that commences after 100 °C until 400 °C (about 19%) is due to the removal of the acid dopant bound to the polyaniline chain and low molecular weight oligomers. A slow and gradual weight loss profile observed starting at 400 °C onwards, represents degradation of the skeletal polyaniline chain structure after the dopant has been removed [18]. Above 700 °C, the results obtained are associated with the residues. The thermogram of IB shows an initial sharp decrease in weight ~ 5-6% within the temperature range of 80–150 °C is attributed to the loss of adsorbed water and interlayer water. A steady weight loss of about 6-7% in the temperature range of 150–800 °C which is attributed to the loss of dehydroxylation caused by breaking of structural hydroxyl groups of the montmorillonite (Fig. 4a). The thermogram of OMIB shows an initial sharp decrease in weight ~ 7% within the temperature range of 80–150 °C is attributed to the loss of adsorbed water and interlayer water. A steady weight loss of about 9% in the temperature range of 150–800 °C which is attributed to the loss of dehydroxylation caused by breaking of structural hydroxyl groups of the montmorillonite and decomposition of the organic moiety present in the interlayers of the clay (Fig. 4b). PANi/IB and PANi/OMIB exhibit similar pattern, with a small variation in degradation temperature. In the first stage, 3-4% weight loss at temperature up to 120 °C is associated with the loss of water molecules [19]. In the second stage corresponding to temperature zone 120-350 °C, the weight loss (about 12-19%) is due to the evolution of thermally labile compounds and the breaking of aliphatic structures with low dissociation bonds in the clay matrix. In the third stage that commences after 350 °C until 700 °C, maximum weight loss occurs (33-38%) due to release of soot particles and the loss of dehydroxylation caused by breaking of structural hydroxyl groups of the clay [20,21]. Above, 700°C gradual decreases were observed due to thermal degradation of mineral matter of clay.

3.5 SEM

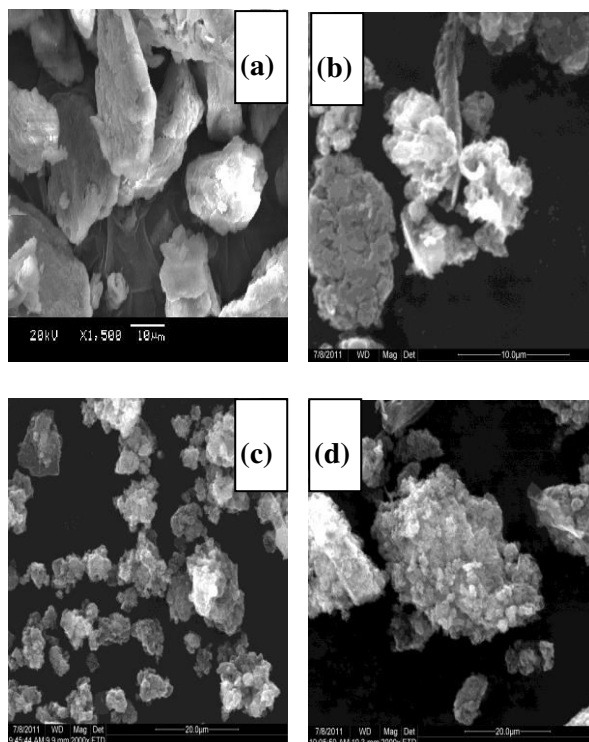


Fig. 5 SEM images of (a) IB, (b) PANi, (c) PANi/IB and (d) PANi/OMIB.

Fig. 5 shows SEM images of IB, PANi, PANi/IB and PANi/OMIB. SEM image of IB (Fig. 5a) shows morphology of clay particles having different irregular shapes, whereas PANi/IB (Fig. 5c) has flake like morphology and PANi and PANi/OMIB have particles of both smaller and bigger sizes with irregular shapes (Fig. 5b&d).

3.6 Electrochemical characterization

Cyclic voltammetry. Fig. 6-8 display the cyclic voltammograms (CV) of PANi, PANi/IB and PANi/OMIB measured in the potential range of -0.2 to 0.6 V employing the scan rates of 10 , 20 , 50 and 100 mVs^{-1} . The corresponding specific capacitances (on y-axis), obtained from the CV curves are also shown. Generally, the charge storage occurs in an electrical double-layer capacitor by electrostatic reversible adsorption of ions of the electrolyte. This type of capacitance behavior gives CV curves close to ideal rectangular shape. But these samples showed CV curves distinctly different from rectangular shape. This pseudocapacitance behavior can be attributed to the charge storage mechanism essentially by redox reactions. There is an inverse relation observed between the scan rate and the total amount of charge stored. In other words, there are kinetic limitations associated with the diffusion of ions through the electrode matrix which limits the full storage of charge at higher scan rates. For example, at 10 mVs^{-1} scan rate, PANi electrode reaches maximum specific capacitance of 457 F g^{-1} while at 20 mVs^{-1} it reaches 388 F g^{-1} , whereas at 10 mVs^{-1} scan rate, PANi/IB electrode reaches maximum specific capacitance of 455 F g^{-1} while at 20 mVs^{-1} it reaches 430 F g^{-1} and at 10 mVs^{-1} scan rate, PANi/OMIB electrode reaches maximum specific capacitance of 415 F g^{-1} while at 20 mVs^{-1} it reaches 323 F g^{-1} . The reduced supercapacitance of PANi/OMIB may be attributed to the presence of

non-conducting cetyltrimethylammonium moiety. From the results, it is clear that PANi/clay nanocomposites show better supercapacitance properties over PANi alone even at higher scan rates.

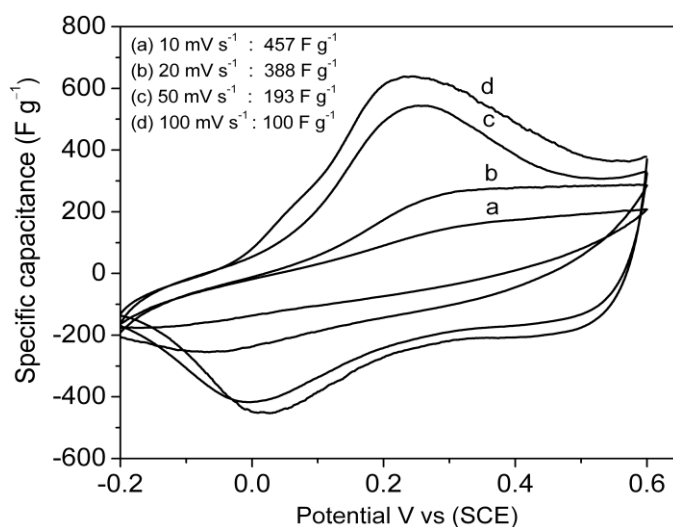


Fig. 6 Cyclic voltammograms of PANi at different scan rates in 0.5 M H₂SO₄ electrolyte.

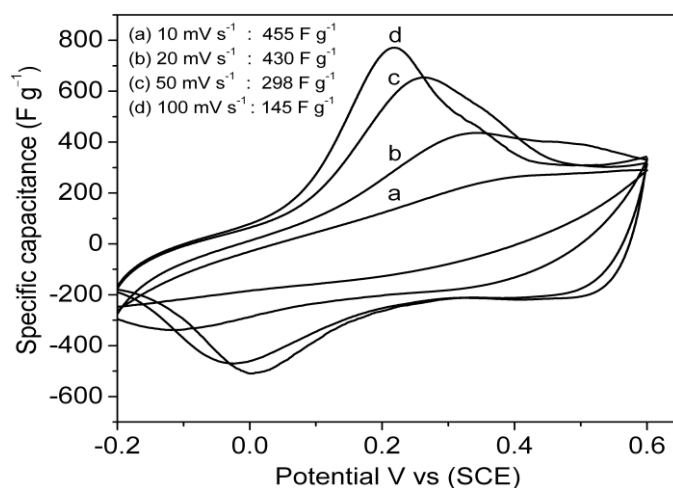


Fig. 7 Cyclic voltammograms of PANi/IB at different scan rates in 0.5 M H₂SO₄ electrolyte.

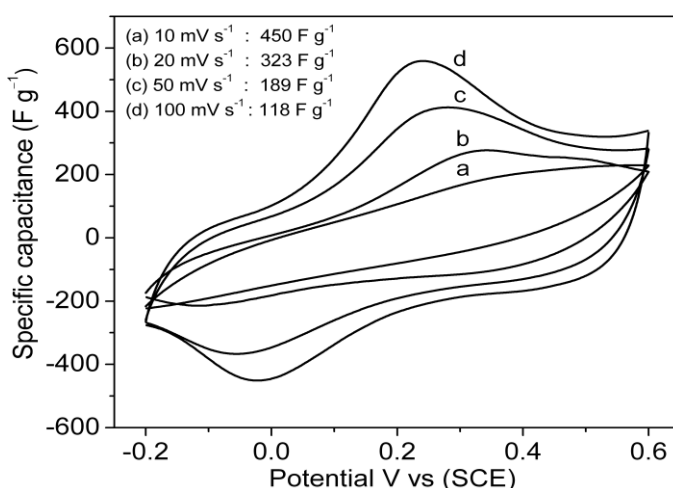


Fig. 8 Cyclic voltammograms of PANi/OMIB at different scan rates in 0.5 M H₂SO₄ electrolyte.

4. Conclusions

Modified clays have been prepared with cetyltrimethyl ammonium bromide. Polyaniline/modified clay and polyaniline/clay nanocomposites have been prepared and characterized for their physico-chemical properties. The polymer/clay nanocomposites are found to be thermally stable compared to pure polyaniline. The electrochemical studies revealed that polyaniline upon modification with clays can be used as supercapacitors for better storage compared to pure polyaniline.

Acknowledgements

This work is funded by the Department of Science and Technology, New Delhi, India, under Fast Track Scheme for Young Scientists (Project No.SR/FTP/CS-11/2006). BVK is grateful to Prof. G. Ranga Rao for his support and encouragement. K. O. Anjana thanks the Indian Academy of Sciences, Bangalore for awarding a summer research fellowship.

References

- [1] Giannelis E P, Krishnamoorti R, Manias E 1999 *Adv. Polym. Sci.* **138** 107
- [2] LeBaron P C, Wang Z, Pinnavaia T J 1999 *Appl. Clay Sci.* **15** 11
- [3] Vaia R A, Price G, Ruth P N, Nguyen H T, Lichtenhan J 1999 *Appl. Clay Sci.* **15** 67
- [4] Biswas M, Ray S S 2001 *Adv. Polym. Sci.* **155** 167
- [5] Aranda P, Ruiz-Hitzky E 1992 *Chem. Mater.* **4** 1395
- [6] Greenland D J 1963 *J. Colloid Sci.* **18** 647
- [7] Blumstein A 1965 *J. Polym. Sci. A* **3** 2665
- [8] Krishnamoorti R, Vaia R A, Giannelis E P 1996 *Chem. Mater.* **8** 1728
- [9] Ray S S, Okamoto M 2003 *Prog. Polym. Sci.* **28** 1539
- [10] Li D, Huang J, Kaner R B 2009 *Acc. Chem. Res.* **42** 135
- [11] Vijayakumar B, Nagendrappa G, Jai Prakash B S 2009 *Catal. Lett.* **128** 183
- [12] Krishna B S, Murty D S R, Jai Prakash B S 2000 *J. Colloid Interface Sci.* **229** 230
- [13] Rees C A, Provis J L, Lukeya G C, van Deventer J S J 2007 *Langmuir* **23** 8170
- [14] Cho M S, Park S Y, Hwang J Y, Choi H J 2004 *Mater. Sci. Engg.: C* **24** 15
- [15] Libert J, Cornil J, dos Santos D A, Bredas J L 1997 *Phy. Rev. B*, **56**(14) 8638
- [16] Glasel H -J, Hartmann E, Hormes J 1999 *J. Mater. Sci.* **34** 1
- [17] Chandrakanthi R L N, Careem M A 2002 *Thin Solid Films* **417** 51
- [18] La Puente G D, Marban G, Fuente E 1998 *J. Anal. Appl. Pyrolysis* **44** 205
- [19] Arenillas A, Rubiera F, Pis J J, Cuesta M J, Iglesias M J, Jimenez A, Suarez-Ruiz I 2003 *J. Anal. Appl. Pyrolysis* **68-69** 371
- [20] Malhotra B D, Chaubey A, Singh S P 2006 *Anal. Chim. Acta*, **578** 59
- [21] Kaushik A, Khan R, Gupta V, Malhotra B D, Singh S P 2009 *J. Nanosci. & Nanotechnol.* **9** 1792

Corrigendum: Polyaniline/clay Nanocomposites: Preparation, Characterization and Electrochemical Properties

B Vijayakumar^{1,*}, K O Anjana² and G Ranga Rao¹

¹ Department of Chemistry, Indian Institute of Technology Madras, Chennai-600036, India

² Department of Chemistry, National Institute of Technology Calicut, Kozhikode-673601, India

E-mail: badathala@rediffmail.com

CORRIGENDUM TO: 2015 IOP Conf. Ser.: Mater. Sci. Eng. **73** 012112

In Experimental, after 2.1 Materials and methods the following text should be inserted:

2.2 Preparation of polyaniline/clay nanocomposites

5 g (13.71 mM) of cetyltrimethylammonium bromide (CTAB) was dissolved in 200 ml of distilled water and 10 g of Indian bentonite (IB) was added. The contents were stirred using a mechanical stirrer for 1 h, the mixture was centrifuged and the centrifugate was discarded. The solid was washed several times with distilled water to remove superficially held adsorbate. The resulting modified clay (OMIB) was dried at 100 °C and ground to a fine powder.

The oxidant solution (0.11 M ammonium persulphate in deionised water) was added dropwise to a mixture of 0.5 g of modified clay, 0.1 M aniline and 0.1 M dopant (*p*-toluene sulphonic acid) in 75 mL deionised water. The reaction was carried out at a temperature of 0-5 °C with ice around the reaction vessel for 12 h under stirring. The controlled low temperature is chosen to prevent high increase in temperature due to the exothermic reactions. The polymer obtained was in the conducting state (emeraldine salt; green colour of doped PANi). The reaction product was separated from the solution by filtration and washed with deionised water several times, followed by washing with ethanol to remove residual monomers. The powder (PANi/OMIB) was then dried at 40 °C under vacuum. Following the same procedure, polyaniline/clay nanocomposite (PANi/IB) and polyaniline (PANi) were prepared by adding parent clay and without clay respectively for comparison.